

Platinum-Free Cathode for Dye-Sensitized Solar Cells Using Poly(3,4-ethylenedioxythiophene) (PEDOT) Formed via Oxidative Molecular Layer Deposition

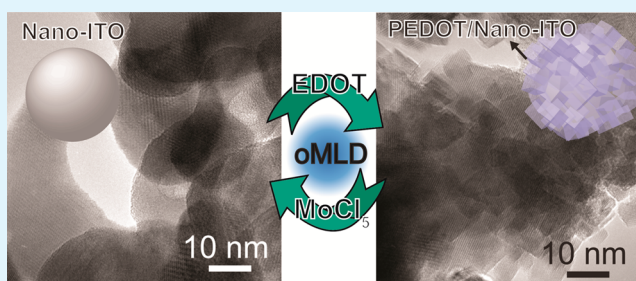
Do Han Kim,[§] Sarah E. Atanasov, Paul Lemaire, Kyoungmi Lee,[§] and Gregory N. Parsons*

Department of Chemical and Biomolecular Engineering, North Carolina State University, 911 Partners Way, Engineering Building I, Raleigh, North Carolina 27606, United States

Supporting Information

ABSTRACT: Thin ~20 nm conformal poly(3,4-ethylenedioxythiophene) (PEDOT) films are incorporated in highly conductive mesoporous indium tin oxide (m-ITO) by oxidative molecular layer deposition (oMLD). These three-dimensional catalytic/conductive networks are successfully employed as Pt-free cathodes for dye-sensitized solar cells (DSSCs) with open circuit voltage equivalent to Pt cathode devices. Thin and conformal PEDOT films on m-ITO by oMLD create high surface area and efficient electron transport paths to promote productive reduction reaction on the PEDOT film. Because of these two synergetic effects, PEDOT-coated m-ITO by oMLD shows power conversion efficiency, 7.18%, comparable to 7.26% of Pt, and higher than that of planar PEDOT coatings, which is 4.85%. Thus, PEDOT-coated m-ITO is an exceptional opportunity to compete with Pt catalysts for low-cost energy conversion devices.

KEYWORDS: PEDOT, molecular layer deposition, PEDOT, dye-sensitized solar cells, cathode



Since initial demonstrations of dye-sensitized solar cells (DSSCs) by Grätzel in 1991, these devices have attracted great interest because of their low cost, high efficiency, and good response to low-intensity light.¹ Dye molecules adsorbed on mesoporous TiO₂ (m-TiO₂) absorb light to excite electrons to the lowest unoccupied molecular orbital. The dye molecules are a key feature in DSSCs because they significantly extend the light absorbance of m-TiO₂ to the visible region (wavelength, $\lambda > 450$ nm), and the excited-state potential of the dye allows rapid charge transfer into the TiO₂ conduction band (CB). From there, they travel through a conductive pathway to the cathode electrode (CE) in contact with the cell electrolyte. The CE is generally coated with platinum (Pt) as an electrocatalyst to promote the rate of charge transfer for electrolyte reduction, which is typically triiodide (I₃⁻) to iodide (I⁻).

Yet, platinum is an expensive precious metal (\$52/g)² and during DSSC operation, it can be released into the liquid electrolyte and transported to the dyed m-TiO₂, promoting the creation of new charge recombination sites.³ Thus, many research teams are exploring alternate CE materials to replace Pt. As a promising alternative to Pt, poly(3,4-ethylenedioxythiophene) (PEDOT) has been extensively investigated because it has high electrical conductivity for a conductive polymer, electrocatalytic activity, and chemical stability, and it facilitates low-temperature processing for flexible DSSCs.⁴ PEDOT can perform as well as, or even better than Pt with careful optimization, especially when the PEDOT is combined with a highly conductive scaffold such as TiN, carbon black,

CuInS₃, CoS, graphene, or carbon nanotubes.^{5–13} Nanostructured PEDOT such as fibers and nanowires are also utilized to provide high surface area as well as efficient electron transport paths for the reduction reaction.^{14,15} Furthermore, TiO₂ particles or polymer binders were combined with PEDOT to form a continuous PEDOT layer on a high-surface-area electrode.^{16,17} Therefore, new processes that can create high-quality PEDOT with uniform, conformal, and well-controlled thickness on complex surfaces will be a significant improvement over current methods for PEDOT cathode fabrication.

Recently, our work reported the synthesis of PEDOT thin films using oxidative molecular layer deposition (oMLD), in which sequential vapor pulses of MoCl₅ as an oxidant and 3,4-ethylenedioxythiophene (EDOT) as a monomer produced highly conformal coating over nanostructures with a high aspect ratio feature.¹⁸ Figure S1a in the Supporting Information (SI) shows a PEDOT film (with darker contrast) coated by oMLD onto the insides of pores in an anodic aluminum oxide membrane. The depth of the coating into the pores corresponds to coverage up to a ~40:1 aspect ratio.

Herein, this work first presents ultrathin and conformal PEDOT films deposited by oMLD on highly conductive mesoporous indium doped oxide (m-ITO), and evaluates its

Received: December 2, 2014

Accepted: February 10, 2015

Published: February 10, 2015

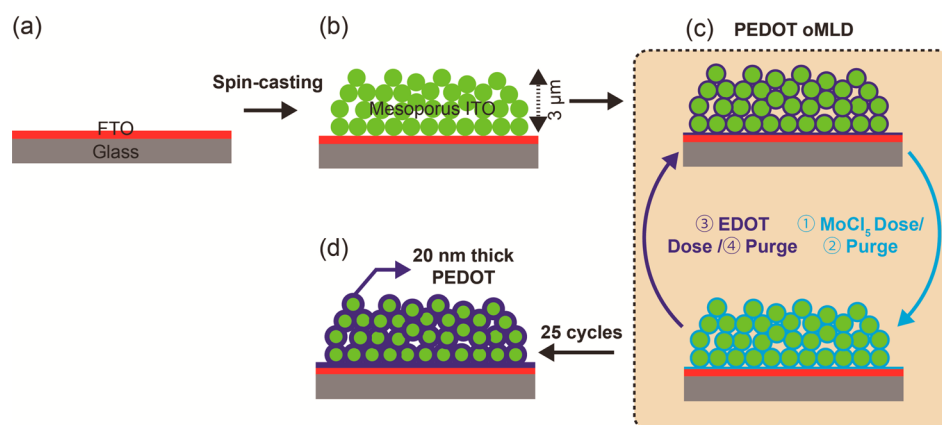


Figure 1. Process scheme for fabricating PEDOT coated m-ITO films for a cathode in DSSCs using oMLD. (a) Cleaned FTO-glass, (b) spun-cast m-ITO with $\sim 3 \mu\text{m}$ thickness on FTO-glass, (c) oMLD of PEDOT on m-ITO, (d) m-ITO coated with $\sim 20 \text{ nm}$ thick PEDOT film after 25 cycles of PEDOT oMLD.

performance as an electrocatalytic cathode in DSSC devices. PEDOT-coated m-ITO (PEDOT/m-ITO) produces high surface area, conductivity, and connectivity of PEDOT within the cathode, thereby promoting efficient electron transport and catalytic activity to reduce I_3^- to 3I^- . Moreover, in oMLD PEDOT/m-ITO, the total material cost of EDOT monomer ($\$0.75/\text{g}$), MoCl_5 oxidant ($\$0.21/\text{g}$), and ITO nanopowders ($\$1.77/\text{g}$) is lower than Pt. oMLD PEDOT is cheaper than even PEDOT ($\$47.4/\text{g}$) in spin-casting so that oMLD PEDOT/m-ITO is superior to both of Pt and spun-cast PEDOT/m-ITO in cost-competitiveness as estimated in Figure S2 in the Supporting Information. Using only $\sim 20 \text{ nm}$ thick PEDOT films on m-ITO, we achieved comparable overall conversion efficiency, 7.18% to 7.26% of conventional Pt. This performance was accomplished without process optimization, showing that PEDOT-coated m-ITO by oMLD is a versatile Pt-free cathode, capable of creating effective catalytic nanostructures for low-cost energy conversion systems.

Figure 1 illustrates a process scheme for CE fabrication for DSSCs including PEDOT oMLD on $\sim 3 \mu\text{m}$ thick m-ITO films. The MoCl_5 vapor is first introduced to the spun-cast m-ITO films (Figure 1b) and adsorbed on the surface in Figure 1c. A purge step then removes unreacted MoCl_5 . A dose of EDOT vapor leads to the surface polymerization forming PEDOT films on the m-ITO, with HCl and excess EDOT as byproduct vapors. The residual gases are purged out by nitrogen, again completing one PEDOT oMLD cycle.¹⁸ The growth rate per cycle at the reactor temperature in this work, $100 \text{ }^\circ\text{C}$, is $\sim 1 \text{ nm/cycle}$ determined at different oMLD temperatures in Figure S1b in the Supporting Information. In this work, total 25 cycles were performed to ensure, at least, $\sim 20 \text{ nm}$ thick PEDOT films on m-ITO (Figure 1d).

TEM measurement in Figure 2 confirms PEDOT films on nano-ITO particles. Figure 2a, b from uncoated m-ITO films show individual nano-ITO particles with diameters of $\sim 40 \text{ nm}$. Figure 2c is a schematic of a nano-ITO particle, based on TEM observations. The particles are well-defined in the images and they show clear diffraction patterns expected for nano-ITO particles. For the PEDOT coated m-ITO in Figure 2d, e, the images show small cubic particles uniformly distributed on the oxide particles as illustrated in Figure 2f. This suggests that on this surface, the hydrophobic PEDOT forms nonwetting 3D nuclei before coalescing into a continuous film.¹⁹

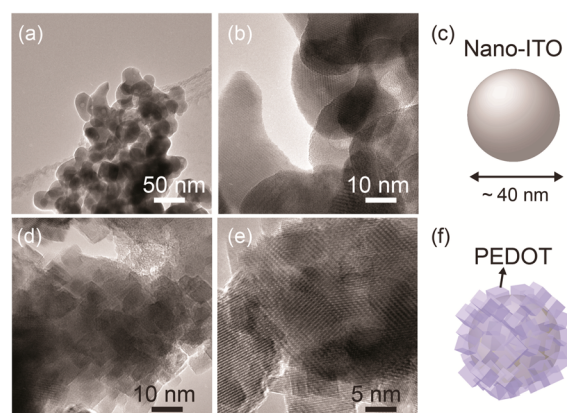


Figure 2. TEM images of (a, b) bare nano-ITO, (d, e) PEDOT-coated m-ITO, where b and e are high-magnification images of a and d, respectively. (c, f) are illustrations of uncoated and PEDOT-coated ITO based on TEM results.

Figure 3 and Figures S3 and S4 in the SI present topological properties of PEDOT-coated m-ITO and compares performance of four different cathodes. The SEM image in Figure 3(a) further confirms that conformal PEDOT films are deposited over the m-ITO particles. The uncoated FTO in Figure S3a in the Supporting Information shows brighter contrast than the m-ITO. After PEDOT oMLD (Figure 3a), both the FTO and ITO layers show the same dark contrast. The dark contrast is consistent with the small mass of atoms such as S in PEDOT compared to Sn in FTO.²⁰ In addition, the lack of SEM contrast in Figure 3a over the entire layer cross-section indicates that PEDOT oMLD uniformly coats both the m-ITO and the FTO surface underneath m-ITO. SEM images showing the top surface of bare and coated m-ITO in the inset of Figure 3a and Figure S3b in the SI respectively show very similar structure, further indicating that the oMLD of PEDOT maintains the underlying porous structure, and does not planarize the surface. This is consistent with the AFM images in Figure 3b. Bare m-ITO, PEDOT-coated FTO-glass, and bare FTO-glass are also exhibited in parallel for comparison in Figure S4a–c in the SI, respectively. As oMLD of PEDOT is deposited on bare FTO and m-ITO, sharp and clear edges of FTO and contours of individual nano-ITO particles appear smooth, which is consistent with the PEDOT-coating. Note, in particular, that the coated m-ITO films in Figure 3b maintain

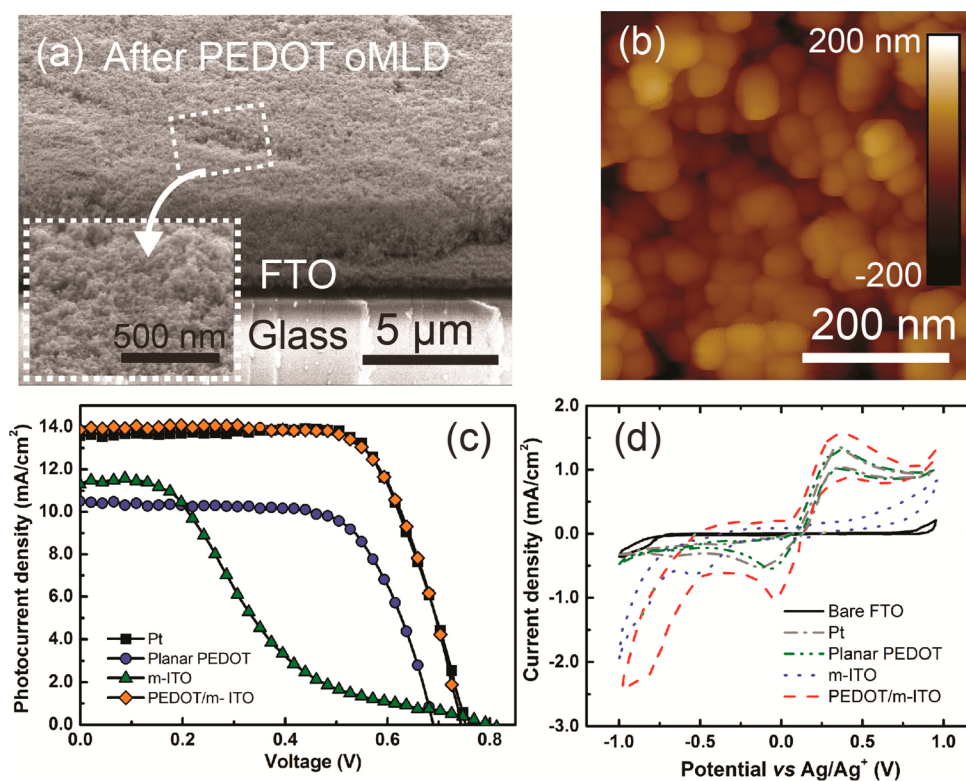


Figure 3. (a) Tilted-view SEM image of PEDOT coated m-ITO on FTO-glass in which the inset presents top surface in dotted box, (b) AFM image of ~ 20 nm thick PEDOT coated m-ITO, (c) photovoltaic performance of representative DSSCs assembled with four different CEs, (d) cyclic voltammograms (CV) obtained after 10 cycles with four CEs in electrolyte containing 10 mM LiI, 1 mM I_2 , and 0.1 M $LiClO_4$ acetonitrile solution at a scan rate 20 mV^{-1} .

Table 1. Performance of DSSCs with Different PEDOT CEs and EIS Parameters Obtained from Symmetric Cells^a

counter electrodes	J (mA/cm^2)	V (V)	FF	η (%)	R_s ($\Omega \text{ cm}^2$)	R_{ct} ($\Omega \text{ cm}^2$)
Pt	13.60	0.75	0.72	7.26 ± 0.11	1.33 ± 0.32	0.89 ± 0.07
planar PEDOT	10.51	0.69	0.67	4.85 ± 0.24	2.81 ± 0.53	36.32 ± 0.08
m-ITO	11.21	0.80	0.24	2.15 ± 0.21	—	—
PEDOT on m-ITO	13.86	0.75	0.69	7.18 ± 0.13	1.92 ± 0.44	0.63 ± 0.12

^aAll DSSCs are fabricated in the same batch for exact comparison; all data are averages of three DSSCs fabricated in the same batch.

open pores without noticeable surface area loss or a top encapsulation layer. This allows the large surface area of the electrode to be maintained in contact with the electrolyte after the PEDOT-coating.

We tested four different cathode configurations to determine the effectiveness of PEDOT: Pt on planar FTO/glass, oMLD PEDOT on planar FTO/glass, oMLD PEDOT on m-ITO/FTO/glass, and bare m-ITO on FTO/glass. Results are shown in Figure 3c and summarized in Table 1. Figure 3(c) shows the resulting current–voltage curves from the fabricated DSSCs. The overall conversion efficiency for the cell using PEDOT coated m-ITO is 7.18%, which is nearly identical to 7.26% measured for the cell using the planar Pt electrode despite of no attempt to optimize oMLD process. Moreover, the efficiency using the nanostructured PEDOT electrode is $\sim 1.5\times$ larger than for the planar PEDOT electrode; all performance parameters (J , V , and FF) are improved. In addition, it is also largely improved by ~ 2.3 times of bare m-ITO in the efficiency, thereby indicating that large surface of m-ITO are effective and pristine m-ITO has the negligible catalytic effect in enhancing performances of DSSCs. Enhanced electrocatalytic performance of PEDOT on m-ITO mainly contributes to improve J , FF

and the improvement in V may also be ascribed to lower sheet resistance and better adhesion between PEDOT and supports such as m-ITO and FTO-glass.^{8,9,12,15,21} Cyclic voltammograms (CV) in Figure 3d make sure that the integration of oMLD PEDOT and m-ITO works in a synergetic manner in regards to high surface area of m-ITO. The two peaks of PEDOT at the negative potential, assigned to the reduction ($I_3^- + 2e \rightleftharpoons 3I^-$) is observed, but the current densities are smaller than Pt because the pristine PEDOT has very slow reduction rate affecting the dye regeneration rate in DSSCs.¹² Yet, when integrated with m-ITO, the current densities increase largely and the peaks become distinct. Meanwhile, in bare m-ITO, the distinctive peaks corresponding to the reduction are not observed even if the integrated area of CV becomes larger due to its high surface area. The PEDOT films contain Mo (< 6 at. %) in oxidized forms, however it does not contribute conductivity and electrocatalytic activity.¹⁸ Therefore, oMLD PEDOT/m-ITO cathode works comparably well, as an alternative Pt cathode, owing to the help of high surface area of m-ITO and catalytic properties of oMLD PEDOT. The PEDOT film is stable, maintaining the conductivity over 2 weeks in ambient

conditions, even if not fully investigated here as a cathode for DSSCs.¹⁸

We also explored the electrochemical characteristics of each cathode with electrochemical impedance spectroscopy (EIS). Symmetric cells were assembled using parallel cathode pairs to avoid possible effects from photoanodes.²² Results are given in Table 1 and Figure S5 in the SI. According to the general transmission line model, the onset of the first semicircle measured at high frequency determines ohmic serial resistance (R_s), and the size of first semicircle is understood as the charge transfer resistance (R_{ct}) of the cathode.²³ The data for two planar electrodes show two semicircles in the impedance traces consistent with the general equivalent circuit for the symmetric cell.²² Fitting the data to this model leads to the R_s and R_{ct} values are given in Table 1. All electrodes show less than 3 Ω cm², series resistance, indicating good contact performance. Compared to Pt, the planar PEDOT shows a larger R_{ct} consistent with a somewhat reduced catalytic efficiency on a per unit surface area basis. Meanwhile, the PEDOT coated m-ITO electrode shows an additional semicircle ascribed to Nernst diffusion that occurs in typical porous systems,²⁴ as expected for this electrode structure. R_{ct} of PEDOT/m-ITO becomes lower than planar Pt and PEDOT. In spite of the lower R_{ct} of PEDOT/m-ITO, the slight lower η % than planar Pt may be ascribed to 3 μ m thick of m-ITO causing slow diffusion rate of ions inside m-ITO layer. This can be managed through device optimization.

In this work, we discovered and demonstrated that mesoporous ITO coated with conformal PEDOT by oxidative molecular layer deposition exhibits good performance as a cathode in functional dye-sensitized solar cells, with performance nearly equivalent to planar Pt coated FTO-glass, even under conditions where the PEDOT was not optimized. The oMLD process facilitates uniform PEDOT film coating onto the complex 3D network of the m-ITO. We expect that the performance of the PEDOT/m-ITO cathodes in DSSCs could be further improved by exploring process parameters such as deposition temperature, PEDOT thickness, m-ITO thickness, and postdeposition treatment, which were not evaluated here. The results show that the porous PEDOT covered cathode, enabled by the sequential surface reactions during the PEDOT oMLD process, can achieve high catalytic activities, using less expensive and more earth-abundant materials. This approach could also extend to high-performance cathodes in other advanced photo- and electrocatalytic devices such as photoelectrochemical and fuel cell systems.

■ ASSOCIATED CONTENT

● Supporting Information

Detailed experimental section and Figure S1–5. This material is available free of charge via the Internet at <http://pubs.acs.org>.

■ AUTHOR INFORMATION

Corresponding Author

*E-mail: parsons@ncsu.edu.

Present Address

[§]D.H.K. and K.L. are currently at Department of Chemical Engineering, Massachusetts Institute of Technology, 77 Massachusetts Avenue, Cambridge, Massachusetts 02139, USA.

Notes

The authors declare no competing financial interest.

■ ACKNOWLEDGMENTS

The authors acknowledge support from the National Science Foundation Grant CBET-1034374.

■ REFERENCES

- (1) O'Regan, B.; Grätzel, M. A Low-Cost, High-Efficiency Solar Cell Based on Dye-Sensitized Colloidal TiO₂ Films. *Nature* **1991**, *353*, 737–740.
- (2) Commodities: Latest Platinum Price & Chart. <http://www.nasdaq.com/markets/platinum.aspx> (accessed May 30, 2014).
- (3) Figgemeier, E.; Hagfeldt, A. Are Dye-Sensitized Nano-Structured Solar Cells Stable? An Overview of Device Testing and Component Analyses. *Int. J. Photoenergy* **2004**, *6*, 127–140.
- (4) Eelschner, A. *PEDOT: Principles and Applications of an Intrinsically Conductive Polymer*; CRC Press: Boca Raton, FL, 2011.
- (5) Yue, G.; Wu, J.; Xiao, Y.; Lin, J.; Huang, M.; Fan, L.; Yao, Y. A Dye-Sensitized Solar Cell Based on PEDOT:PSS Counter Electrode. *Chin. Sci. Bull.* **2013**, *58*, 559–566.
- (6) Thompson, S. J.; Pringle, J. M.; Zhang, X. L.; Cheng, Y.-B. A Novel carbon–PEDOT Composite Counter Electrode for Monolithic Dye-Sensitized Solar Cells. *J. Phys. Appl. Phys.* **2013**, *46*, 024007.
- (7) Shin, H.-J.; Jeon, S. S.; Im, S. S. CNT/PEDOT Core/shell Nanostructures as a Counter Electrode for Dye-Sensitized Solar Cells. *Synth. Met.* **2011**, *161*, 1284–1288.
- (8) Zhang, Z.; Zhang, X.; Xu, H.; Liu, Z.; Pang, S.; Zhou, X.; Dong, S.; Chen, X.; Cui, G. CuInS₂ Nanocrystals/PEDOT:PSS Composite Counter Electrode for Dye-Sensitized Solar Cells. *ACS Appl. Mater. Interfaces* **2012**, *4*, 6242–6246.
- (9) Xu, H.; Zhang, X.; Zhang, C.; Liu, Z.; Zhou, X.; Pang, S.; Chen, X.; Dong, S.; Zhang, Z.; Zhang, L.; et al. Nanostructured Titanium Nitride/PEDOT:PSS Composite Films As Counter Electrodes of Dye-Sensitized Solar Cells. *ACS Appl. Mater. Interfaces* **2012**, *4*, 1087–1092.
- (10) Xiao, Y.; Lin, J.-Y.; Tai, S.-Y.; Chou, S.-W.; Yue, G.; Wu, J. Pulse Electropolymerization of High Performance PEDOT/MWCNT Counter Electrodes for Pt-Free Dye-Sensitized Solar Cells. *J. Mater. Chem.* **2012**, *22*, 19919–19925.
- (11) Kitamura, K.; Shiratori, S. Layer-by-Layer Self-Assembled Mesoporous PEDOT–PSS and Carbon Black Hybrid Films for Platinum Free Dye-Sensitized-Solar-Cell Counter Electrodes. *Nanotechnology* **2011**, *22*, 195703.
- (12) Sudhagar, P.; Nagarajan, S.; Lee, Y.-G.; Song, D.; Son, T.; Cho, W.; Heo, M.; Lee, K.; Won, J.; Kang, Y. S. Synergistic Catalytic Effect of a Composite (CoS/PEDOT:PSS) Counter Electrode on Triiodide Reduction in Dye-Sensitized Solar Cells. *ACS Appl. Mater. Interfaces* **2011**, *3*, 1838–1843.
- (13) Hong, W.; Xu, Y.; Lu, G.; Li, C.; Shi, G. Transparent graphene/PEDOT–PSS Composite Films as Counter Electrodes of Dye-Sensitized Solar Cells. *Electrochem. Commun.* **2008**, *10*, 1555–1558.
- (14) Trevisan, R.; Döbbelin, M.; Boix, P. P.; Barea, E. M.; Tena-Zaera, R.; Mora-Seró, I.; Bisquert, J. PEDOT Nanotube Arrays as High Performing Counter Electrodes for Dye Sensitized Solar Cells. Study of the Interactions Among Electrolytes and Counter Electrodes. *Adv. Energy Mater.* **2011**, *1*, 781–784.
- (15) Lee, T. H.; Do, K.; Lee, Y. W.; Jeon, S. S.; Kim, C.; Ko, J.; Im, S. S. High-Performance Dye-Sensitized Solar Cells Based on PEDOT Nanofibers as an Efficient Catalytic Counter Electrode. *J. Mater. Chem.* **2012**, *22*, 21624–21629.
- (16) Chiang, C.-H.; Wu, C.-G. High-Efficient Dye-Sensitized Solar Cell Based on Highly Conducting and Thermally Stable PEDOT:PSS/glass Counter Electrode. *Org. Electron.* **2013**, *14*, 1769–1776.
- (17) Maiaugree, W.; Pimanpang, S.; Towannang, M.; Saekow, S.; Jarernboon, W.; Amornkitbamrung, V. Optimization of TiO₂ Nanoparticle Mixed PEDOT–PSS Counter Electrodes for High Efficiency Dye Sensitized Solar Cell. *J. Non-Cryst. Solids* **2012**, *358*, 2489–2495.
- (18) Atanasov, S. E.; Losego, M. D.; Gong, B.; Sachet, E.; Maria, J.-P.; Williams, P. S.; Parsons, G. N. Highly Conductive and Conformal Poly(3,4-Ethylenedioxythiophene) (PEDOT) Thin Films via Oxidative Molecular Layer Deposition. *Chem. Mater.* **2014**, *26*, 3471–3478.

- (19) George, S. M. Atomic Layer Deposition: An Overview. *Chem. Rev.* **2010**, *110*, 111–131.
- (20) Kim, K. H.; Akase, Z.; Suzuki, T.; Shindo, D. Charging Effects on SEM/SIM Contrast of Metal/Insulator System in Various Metallic Coating Conditions. *Mater. Trans.* **2010**, *51*, 1080.
- (21) Papageorgiou, N. Counter-Electrode Function in Nanocrystalline Photoelectrochemical Cell Configurations. *Coord. Chem. Rev.* **2004**, *248*, 1421–1446.
- (22) Hauch, A.; Georg, A. Diffusion in the Electrolyte and Charge-Transfer Reaction at the Platinum Electrode in Dye-Sensitized Solar Cells. *Electrochim. Acta* **2001**, *46*, 3457–3466.
- (23) Fabregat-Santiago, F.; Bisquert, J.; Garcia-Belmonte, G.; Boschloo, G.; Hagfeldt, A. Influence of Electrolyte in Transport and Recombination in Dye-Sensitized Solar Cells Studied by Impedance Spectroscopy. *Sol. Energy Mater. Sol. Cells* **2005**, *87*, 117–131.
- (24) Roy-Mayhew, J. D.; Bozym, D. J.; Punckt, C.; Aksay, I. A. Functionalized Graphene as a Catalytic Counter Electrode in Dye-Sensitized Solar Cells. *ACS Nano* **2010**, *4*, 6203–6211.